

REVIEW ARTICLE

Nuclear physics with RI Beam Factory

Hiro Yoshi Sakurai

*Department of Physics, University of Tokyo, 7-3-1 Hongo Bunkyo-ku, Tokyo 113-0033, Japan
RIKEN Nishina Center for Accelerator-Based Science 2-1 Hirosawa Wako Saitama 351-0198, Japan
E-mail: sakurai@ribf.riken.jp*

Received August 14, 2018; accepted August 25, 2018

Research activities of nuclear physics at Radioactive Isotope Beam Factory over 10 years are reviewed and future directions are also discussed. Conceptual ideas in designing the facility as well as experimental devices are introduced. Special emphasis is given to highlighted results obtained at RIBF.

Keywords radioactive isotope beams, heavy-ion accelerator facility, in-flight production, experimental devices and techniques, storage rings, r -process path, nuclear waste problems

PACS numbers 21.10.-k, 21.30.-x, 21.65.+f, 26.30.-k, 28.41.Kw, 29.20.-c, 20.20.db, 29.25.Rm, 29.30.-h

Contents

1	Introduction	
2	Overview of the RIBF facility	
2.1	RI beam production system	
2.2	Experimental devices and nuclear physics programs	
3	Highlighted results at RIBF	
3.1	Nihonium and mass spectroscopy	
3.2	Discovery of new isotopes	
3.3	Shell evolution – New magicity and magicity loss	
3.4	Impacts on the r -process path	
3.5	Nucleon correlation	
3.6	Reaction study with long-lived fission products in nuclear wastes	
4	Summary and outlook	
	Acknowledgements	
	References	

based on high energy RI beams.

The concept of RIBF was firstly proposed by Y. Yano and M. Ishihara in 1992, just after the RIKEN Ring Cyclotron (RRC) project was completed. The idea stemmed from significant expansion of sciences with radioactive isotope (RI) beams produced at in-flight separator. At the in-flight separator “RIPS” [2] coupled with RRC, the nuclear structure and nuclear astrophysics were studied with light and intense RI beams via developments of several spectroscopy techniques with inverse kinematics. These activities have been significantly expanded to medium and heavy mass region at the new facility of RIBF.

The first international advisory committee was organized in 1994 according to a suggestion of Prof. Arima as the President of RIKEN. Next year, the project was officially approved by the Government.

Under the construction phase of RIBF, the existing facility of RRC were upgraded step by step. One of the great improvements was intensity and energy upgrade of heavy-ion linear accelerator RILAC by installing a frequency variable RFQ, and also by additional RF cavities of CNS, Univ. of Tokyo. The RILAC upgrade created a great opportunity for production of super heavy elements via cold fusion reaction. Since 2004 to 2012, three events of the Element 113 were successfully observed and identified [3–5]. and the naming right was given to K. Morita and his colleagues, who named the new element “Nihonium (Nh)”.

Meanwhile, construction of new cyclotrons and a new in-flight separator was smoothly conducted and the first beam was successfully accelerated at and delivered from a main cyclotron, “Superconducting Ring Cyclotron

1 Introduction

The “Radioactive Isotope Beam Factory (RIBF)” is one of the leading facilities in the world [1], aiming at major scientific goals; i) to discover new quantum phenomena associated with a large isospin asymmetry through investigating nuclear structure in very neutron-rich nuclei, ii) to elucidate the r -process path in explosive processes of the universe, and iii) to develop new applied sciences

*Special Topic: Simplicity, Symmetry, and Beauty of Atomic Nuclei (Eds. Jie Meng, Takaharu Otsuka & Yu-Min Zhao).

(SRC)” in 2006 [6]. Next year, RIBF started in operation, and the first experiment to search for new isotopes was conducted at the new in-flight separator “BigRIPS” [7] with a 345A MeV uranium beam from SRC and two new isotopes were successfully found [8]. Since then, experimental devices coupled with radioactive isotope (RI) beams produced at BigRIPS were successively constructed, and scientific outputs have been produced under international collaborations formed at each device or newly developed detectors [9].

In this review paper, overview of the accelerator complex of RIBF, experimental devices and programs at each device are given. Then research highlights are introduced for results obtained at the new facility, not for activities at the old facility of RIBF such as a CNS project “CRIB” [10] and a KEK project “KISS” [11]. Finally, summary and outlook are described.

2 Overview of the RIBF facility

The “Radioactive Isotope Beam Factory (RIBF)” is the third generation in-flight facility [12] to deliver intense radioactive isotope (RI) beams based on the high-intensity heavy-ion accelerator complex, as shown in Fig. 1. A key concept in designing RIBF was to achieve large dynamic ranges in terms of RI beam intensities, RI species and a large diversity of experimental programs. In this section, we would give an overview of RI beam production scheme at RIBF and introduce experimental devices and programs with the RI beams available at RIBF.

2.1 RI beam production system

To access nuclei far from the stability line, especially for neutron-rich nuclei, the RIBF facility is highly optimized for in-flight production of fission fragments via a U beam. “Super-conducting Ring Cyclotron (SRC)” (see Fig. 2) in the accelerator complex delivers a 345 MeV/u U beam [6]. The U nuclide is converted at a target to

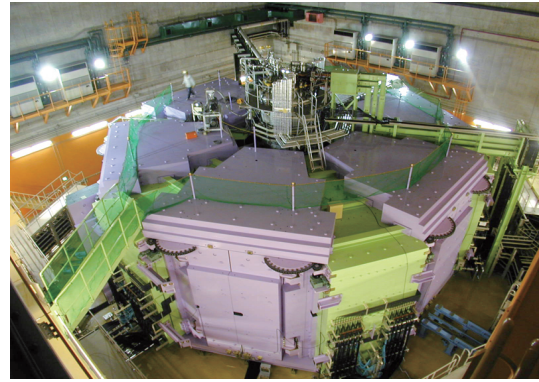


Fig. 2 Photo of Superconducting Ring Cyclotron (SRC) (Courtesy of RIKEN). SRC ($K = 2600$ MeV) is the first ring cyclotron with superconducting magnets.

fission fragments. An in-flight separator “BigRIPS” (see Fig. 3) was designed to collect about 50% of fission fragments produced at the target and separate nuclei of interest [7]. The RI beams are then delivered to several experimental devices. Yield-optimum beam energy of RI beams is about 200–250A MeV.

The accelerator complex has a few acceleration modes which depend on mass number of primary beams [6]. Year-by-year the primary beam intensity has been increased, and in 2017, the U beam intensity is beyond 60 pnA. Not only fission but also fragmentation reaction are very useful to study exotic nuclei. The flag-ship primary beam species for fragmentation reaction are ^{18}O , ^{48}Ca and ^{70}Zn for neutron-rich nuclei, and ^{78}Kr and ^{124}Xe for neutron-deficient nuclei. It should be noted that a polarized deuteron beam is also delivered from SRC, where an excellent single turn extraction is achieved.

Particle identification for secondary beams is made at the second stage of BigRIPS. The second stage has ex-

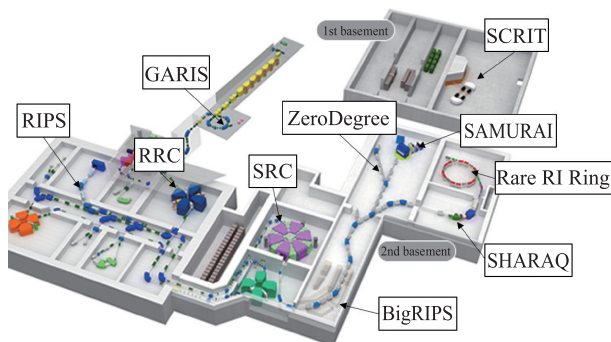


Fig. 1 Facility layout of RIBF (Courtesy of RIKEN).



Fig. 3 Photo of a part of BigRIPS in-flight separator (Courtesy of RIKEN). RI beams produced at the first stage of BigRIPS (left, behind the concrete wall) are transmitted to the second stage and the beams identified at the second stage are delivered to experiment sites.

cellent resolution of momentum and TOF and because of the nice performances, charge-states of the secondary beams could be identified, too, via very precise $B\rho$ -TOF measurement [7]. Further purification of secondary beams is possible at the second stage.

2.2 Experimental devices and nuclear physics programs

In 2013, all the experimental devices proposed have been completed, and have been ready to produce massive data.

Reaction study for the nuclear structure is one of the major projects at RIBF. To accept any kinds of reaction study, RIBF has three large spectrometers; ZeroDegree Spectrometer [7], SAMURAI [13] and SHARAQ [14]. These spectrometers are complementary with each other in terms of momentum resolution and acceptance, and solid angle.

Unique devices for specific programs are BigDPOL for polarized deuteron beams, Rare-RI Ring for mass measurements [15], SCRIT system for charge form factor measurements [16, 17]. SLOWRI gas catcher system [18] was constructed to deliver very slow RI beams.

2.2.1 BigDPOL

A unique study for three nucleon force is organized at BigDPOL. This study is based on precise cross section and analyzing power measurements of deuteron and proton elastic scattering with a 190, 250 and 294A MeV polarized deuteron beam. In this experiment, the AVF-RRC-SRC acceleration scheme was applied to accelerate the polarized beams. A single turn extraction of the beam was successfully achieved. The newly constructed polarimeter BigDPOL located at the beam transport line from the exit of SRC to a location of production target at BigRIPS was used to obtain a complete set of tensor analyzing power in the scattering [19–21].

2.2.2 BigRIPS

With the BigRIPS separator only, several unique programs have been conducted. One of the programs is to search for new isotopes towards the drip lines. According to the high performances of particle identification at

BigRIPS, very clear, unambiguous and background-free particle identification is achieved. This program is very essential in two aspects. Firstly, the program gives evidence of particle stability of the newly found isotopes. Secondly, the program gives production cross sections for exotic nuclei, which help in estimating RI beam intensities for coming experiment programs. Since 2007, new isotopes were found and reported by several works [8, 22, 24, 25]. New isomers were also found with clover-Ge detectors for isomer-tagged particle identification [26].

The second program is total interaction cross section measurement based on transmission method, which is very efficient to obtain information on size of exotic nuclei [27, 28]. In this program, the secondary target was installed at the intermediate dispersive focal plane in the second stage of BigRIPS (F5).

A novel technique to produce spin-aligned RI beams via two-step fragmentation reactions were successfully developed at BigRIPS [29]. The new technique stems from a new idea that spin-aligned RI beams are efficiently produced at F5 with dispersion matching technique. This technique has a great potential to measure electromagnetic moments of exotic nuclei.

The other type of programs running at BigRIPS is to study deeply bound pionic states [30], where the atomic states were made via (d, ^3He) reaction with a primary deuteron beam at 500 MeV. High resolution was achieved by employing dispersion matching mode and a large angular acceptance of BigRIPS made it possible to observe not only s -orbit but also p -orbit states.

2.2.3 ZeroDegree Spectrometer

The ZeroDegree Spectrometer (ZDS) is a beam-line spectrometer and appropriate for inclusive- and semi-exclusive experiments, where ejectiles scattered at forward angles via reactions are identified by ΔE -TOF- $B\rho$ - E measurements (see Fig. 4). ZDS commissioning was organized and detectors and optical conditions were examined in 2008. ZDS is also used as a beam transport line to a decay spectroscopy station.

Experimental programs at ZDS are focusing the struc-



Fig. 4 Photo of ZeroDegree Spectrometer (Courtesy of RIKEN).

ture study with low momentum and low energy transfer reactions, such as elastic or inelastic scattering, one- or two-nucleon knock-out reactions, fragmentation reactions. In 2008, the first spectroscopic experiments for exotic nuclei were organized for the island-of-inversion region. Since then, several experimental programs have been organized; in-beam gamma spectroscopy, missing mass spectroscopy and decay spectroscopy.

In-beam gamma spectroscopy at ZDS is one of very efficient programs for the nuclear structure study for a global survey to find out exotic natures in neutron-rich nuclei. As described in Ref. [31], combination between a high efficient NaI array “DALI2” [32] and thick secondary targets has made it possible to access very neutron-rich nuclei with fast RI beams. Since 2008, several types of reactions, inelastic scattering, Coulomb excitation, fragmentation reactions have been applied to obtain exotic structure of neutron-rich nuclei [33–62]. Interestingly, thanks to the intense RI beams, a new isotope was successfully found and identified at ZDS during an in-beam gamma program [63]. A campaign program to search for the first excited states in even-even nuclei with the MINOS target [64] (SEASTAR collaboration) was organized since 2014 to 2017. The first and second phases of the program were conducted at ZDS [65–72]. The third one was organized at SAMURAI as described in Section 2.2.4.

Missing mass spectroscopy with a Si-CsI array MUST2 [73] was once applied for study of excited states in ^{24}O [74].

Decay spectroscopy has been organized at the end of ZDS [75]. The first experiments of decay spectroscopy with four clover-Ge arrays were conducted to access neutron-rich $A\sim 110$ nuclei [76–79], which were produced with a uranium beam. According to the success of the first decay spectroscopy, the EURICA collaboration [80] was started in 2012 to conduct γ spectroscopy by installing the Euro Cluster array. Multitude of decay data were obtained from 2013 to 2016 for both neutron-rich nuclei and neutron-deficient nuclei [81–124]. A part of the campaign was organized with LaBr_3 detectors additionally combined with the EURICA setup to measure lifetimes of excited states [92]. It should be noted that in the EURICA programs new isotopes were discovered because of rather long term data-acquisition time at one $B\rho$ setting of BigRIPS [100, 101, 104, 112, 120, 121].

After the EURICA campaign, a new program BRIKEN has been launched to measure beta-delayed neutron emission probability [125]. The delayed neutrons are measured with a large-size ^3He proportional counter array of which total neutron detection efficiency is as high as 70%. The physics runs have been started since 2017.

Since 2014, ZDS has been utilized for spallation reac-

tion study with radioactive isotope beams, where ZDS serves particle identification for reaction products [126–128].

2.2.4 SAMURAI

SAMURAI [13] is a versatile spectrometer with a large-acceptance in both momentum and solid angle to exclusively measure reaction products in projectile-rapidity frame, mainly through observing particle-unbound states via invariant mass method. The major part of the spectrometer is a superconducting magnet with a large gap (80 cm) and a bending power of 7 Tm.

Since commissioning run of SAMURAI in 2012, SAMURAI has served for physics runs [129–131]. Three types of experiment programs have been conducted. The first type is observation of unbound ground or excited states in very neutron rich nuclei at or beyond the drip line. The observation is based on the invariant mass spectroscopy, which is sometimes coupled with measurements of de-excited gamma rays by DALI2 [32]. The second type is kinematically complete measurement to detect particle-decay with invariant mass method, and to detect recoil particles from target with missing mass method. (p, n) and (p, pn) reactions were employed for ^{132}Sn and ^{11}Li , respectively, where recoil neutrons were measured with the WINDS plastic array [132]. The third one is reaction study with heavy-ion collisions by installing a TPC in the gap of the SAMURAI magnet under the S π RIT collaboration [133].

In 2015–2017, a neutron detector array NeuLAND was installed to enhance multi-neutron detection efficiency, and a campaign program with NeuLAND was organized.

In 2017, the third phase of SEASTAR program was conducted at SAMURAI. Due to the wide momentum acceptance, one $B\rho$ setting at SAMURAI accepted reaction products in a wide dynamic range of Z and A . Bunch of excited states in exotic nuclei were successfully observed.



Fig. 5 Photo of SAMURAI spectrometer (Courtesy of RIKEN). A large-gap super-conducting magnet are combined with standard detectors; large size drift chambers, hodoscopes and neutron TOF detector array.



Fig. 6 Photo picture of SHARAQ spectrometer (Courtesy of CNS, Univ. of Tokyo). RI beams through a special beam line designed to achieve a dispersion matching optics mode come from left.

2.2.5 SHARAQ

The SHARAQ spectrometer [14], which is operated by CNS, University of Tokyo, has a high momentum resolution of 15 000 (see Fig. 6). To achieve the high resolution, a beam transport line from BigRIPS to SHARAQ was specially designed to realize dispersion matching mode. With the advent of this spectrometer, a new type of missing mass spectroscopy, where an RI beam is utilized as a probe to investigate stable nuclei via standard kinematics, is applied to investigate phenomena such as the double Gamow-Teller states, which have been hardly accessible with reactions induced by stable beams.

A commissioning experiment was performed in 2009, and since then, several programs have been conducted via (t , ${}^3\text{He}$) reaction [134], (${}^8\text{He}$, ${}^8\text{Be}$) reaction [135], (${}^{12}\text{N}$, ${}^{12}\text{C}$) reaction [136], and (p , $2p$) reaction [137]. According to the high momentum resolution, mass measurement for light and neutron-rich nuclei was performed, too, based on precise $B\rho$ -TOF measurement [138].

2.2.6 Rare-RI Ring

Rare-RI Ring (R^3) (see Fig. 7) is a storage ring to measure mass of exotic nuclei by TOF measurement based



Fig. 7 Photo of Rare-RI Ring (Courtesy of RIKEN) dedicated to mass measurement for exotic nuclei with isochronous mode via individual injection scheme.

on isochronous mode realized in the ring [15]. R^3 has a unique scheme of individual injection. In this scheme, kicker magnet is switched on at every time when a nucleus of interest comes at BigRIPS. This scheme is fit for c.w. beam of cyclotron, and leading to efficient mass measurements for exotic nuclei. R^3 is designed to have mass resolution of 10^{-6} .

Commissioning runs at R^3 were successfully organized to confirm individual injection mode and to test quality of isochronous optics. Since 2018, physics runs would start the measurement for exotic nuclei related to the r -process path.

2.2.7 SCRIT

The SCRIT facility (see Fig. 8) aims to measure charge form factor of exotic nuclei by electron elastic scattering [16, 17]. A novel technique of Self-Confining RI Target (SCRIT) has been developed for about two decades. A pulsed beam of RI produced at an electron-driven ISOL is transferred into a SCRIT target section in an electron storage ring. A limit of collision luminosity is estimated to be $10^{-27} \text{ cm}^{-2} \cdot \text{s}^{-1}$.

Very recently, a test with a stable ${}^{132}\text{Xe}$ nucleus was successfully organized to obtain its charge form factor for the first time [139].



Fig. 8 Picture of SCRIT system which has been developed to measure charge-form factor of exotic nuclei (Courtesy of RIKEN).

3 Highlighted results at RIBF

In this section, highlighted results obtained at RIBF are introduced in physics point of views.

3.1 Nihonium and mass spectroscopy

Super-heavy element (SHE) science was conducted at “GAs-filled Recoil Ion Separator (GARIS)” [140], which is designed to collect and separate fusion products.

According to energy upgrade of a linear accelerator RILAC, as well as intensity upgrade given by a frequency variable RFQ at RILAC, GARIS was moved to be coupled with RILAC.

In 2004 and 2005, the Element 113 was successfully produced and identified [3, 4]. In 2012, the third event was found, where seven consecutive alpha decays to known nuclides were observed very clearly [5].

In addition to GARIS, “GARIS-II” [141] has been constructed and been coupled with RILAC, too. GARIS-II has a larger acceptance than GARIS and is optimized for hot-fusion reactions. With all these GARIS-devices combined, new elements such as 119th and 120th will be searched for.

Very recently mass spectroscopy at GARIS-II was successfully conducted with multi-reflection TOF technique [142], and showing the deformed $N = 152$ shell closure for Md and Lr.

3.2 Discovery of new isotopes

As described in Sections 2.2.2 and 2.2.3, more than 130 new isotopes have been discovered at RIBF. In this section, a few highlighted results are introduced and underlying physics are discussed.

One of the interesting results is the discovery of ^{72}Rb [120], of which lifetime of the ground state may be longer than that of the neighboring nucleus ^{73}Rb . Thus, ^{72}Rb comes up on the nuclear chart as a “sandbank” beyond the proton drip-line, as shown in Fig. 9. In general, because of the pairing effect, binding energy of odd-even nuclei is larger than that of odd-odd nuclei. However, the finding is contradictory with the general rule. The nucleus ^{72}Rb is a odd-odd nucleus, of which proton- and neutron-numbers are 37 and 35, respectively. Thus, it is very challenging to find out the reason why the odd-odd nucleus of ^{72}Rb is more stable than the odd-even nucleus of ^{73}Rb . Future investigation for the reason by mass measurement and reaction study may give hints for a proton-neutron pairing, or “deuteron clustering” inside a nucleus. So far along the $N = Z$ line, many efforts have been made to find out or predict proton-neutron pairing effects. However, concerning the stability, $N = Z$ nuclei are known to have so called “Wigner effect” which dis-

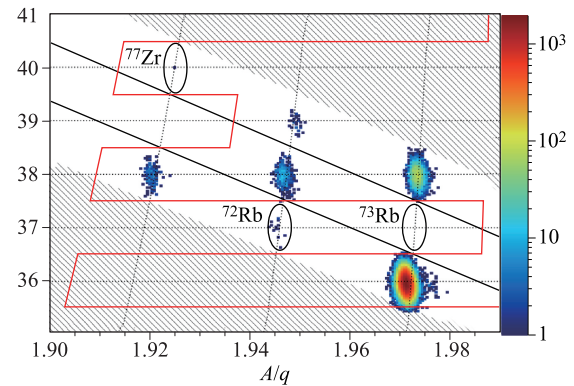


Fig. 9 Two dimensional plot for particle identification, which shows ^{72}Rb events and lack of ^{73}Rb events, taken from Ref. [120].

turbes clear observation or discussion about the proton-neutron pairing. Thus, ^{72}Rb may become a good “laboratory” for such a study in future.

The second interesting finding is the particle stability of ^{60}Ca and other neighboring nuclei [25]. The obtained results give a key discriminator for theoretical models, and the models which predict the finding predict that the neutron drip-line nucleus in the Ca isotopes is ^{70}Ca . On the other hand, theoretical works, which include three-body effects, predict that the Ca isotope chain is rather short as like that of the O isotopes. At present, experimental works just reached at ^{60}Ca . Future works associated with N -dependences of single particle energy of $g_{9/2}$ are essentially important in terms of the Ca drip-line.

3.3 Shell evolution – New magicity and magicity loss

Shell evolution is one of the major subjects at RIBF, and the nuclear structure study has been organized with all of spectroscopy techniques applied at RIBF. Special emphasis is given here for new magicity and magicity loss found at RIBF.

3.3.1 Beyond the island of inversion and deformed halo nuclei

The island of inversion region at $Z \sim 12$ and $N \sim 20$ is a pilot region for the nuclear structure study with respect to large isospin asymmetry. In early 70’s, binding energies of neutron-rich Na isotopes, and energy of the first excited state of ^{32}Mg were measured at CERN ISOLDE, and the isotopes in the region were found to have large deformation in spite of magic number of 20. According to the advent of in-flight facilities in 80-90’s and of post-accelerated beams at ISOL in 00’s, the nuclear structure in the region was extensively studied with a variety of reactions.

At RIBF, the island-of-inversion region has been in-

investigated since the first spectroscopy was organized in 2008. The first attempt was made in a region newly explored at RIBF to survey the ground state collectivity through observation of 2^+ and/or 4^+ states in even-even isotopes via in-beam gamma spectroscopy. The data obtained for ^{32}Ne [33], $^{36,38}\text{Mg}$ [41] and ^{42}Si [37] showed interesting phenomena. First of all, ^{32}Ne is found more deformed than ^{30}Ne . Secondly, as shown in Fig. 10, degree of deformation in the neutron-rich Mg isotopes does not change dramatically as a function of N , but is almost constant from $N = 22$ to 26. Thirdly, ^{42}Si with $N = 28$ has large deformation, and degree of deformation in the Si isotopes is increased as a function of N . Recent invariant mass spectroscopy successfully obtained 2^+ energy for ^{26}O [129], which is rather low compared with that of ^{24}O .

All the above results combined show that the deformation region is not like an “island”, but expanding toward $Z = 8$ and also $N = 28$, like a “peninsula”, and magicity of both $N = 20$ and 28 is lost in the light and neutron-rich region. The findings suggest that sd- and pf-shells are completely mixed together in the neutron-rich Ne, Mg and Si isotopes.

The other surprising result obtained in the deformation region is discovery of the neutron-halo structure in ^{31}Ne [27, 34, 44] and ^{37}Mg [28, 47]. These data were taken via inclusive Coulomb breakup method and total interaction cross section measurements. Both data showed an increase of the cross sections at ^{31}Ne and ^{37}Mg .

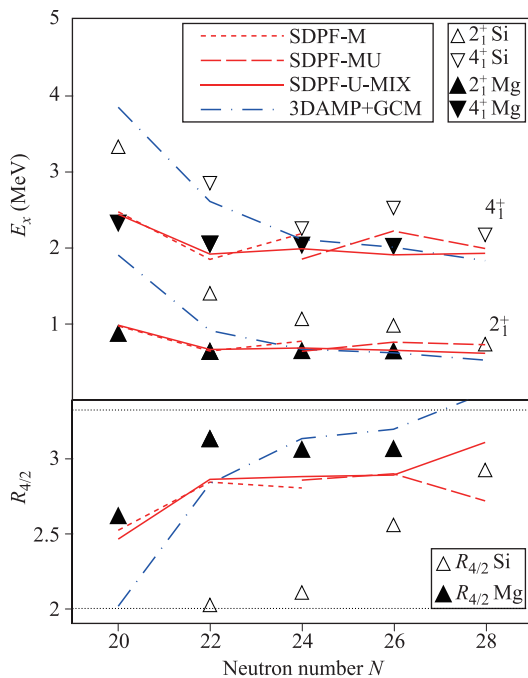


Fig. 10 Energy of 2^+ and 4^+ excited states in neutron-rich Mg isotopes [41].

In general, halo formation needs two conditions. One is low binding energy of valence neutrons and the other is low orbital angular momentum of valence neutrons (ℓ). Both conditions are necessary to give a long tail of wave function. In the case of ^{31}Ne and ^{37}Mg , the binding energies of one valence neutron are well below 1 MeV. Then, a question arises about ℓ .

According to discussions in Ref. [27, 28], the formation mechanism could be naturally explained on the basis of Nilsson-diagram. For example, when ^{31}Ne is well deformed, candidates of Nilsson orbits for the valence neutron are $1/2[330]$, $3/2[321]$ and $1/2[200]$. These Nilsson orbits are described with linear combinations of spherical orbits. When binding energy is decreased, low ℓ orbits become dominant. Because of this binding energy dependence of ℓ components, a Nilsson orbit originating from f ($\ell = 3$) or d ($\ell = 2$), for example, is becoming $\ell = 1$ or $\ell = 0$ dominant in the case of weak binding of the orbits.

The above simple picture could be also applied to halo formation mechanism of ^{11}Li and ^{11}Be . In the case of one neutron halo nucleus ^{11}Be , the binding energy of one valence neutron is about 500 keV, and the ground state spin parity is not $\frac{1}{2}^-$ but $\frac{1}{2}^+$. Because of the positive parity of the ground state, many discussions assumed that 2s orbit becomes more stable than the $1p_{1/2}$ orbit due to some reasons. However, ^{10}Be and ^{12}Be are well known to have large deformation, thus discussions based on the Nilsson picture could be made. Because of large deformation of ^{11}Be , three Nilsson orbits are generated from $d_{5/2}$ and one of them ($1/2[220]$) is lower than $p_{1/2}$. Due to the low binding energy, the $1/2[220]$ orbit becomes s-wave dominant though the origin of the $1/2[220]$ orbit is d-wave. The halo structure of ^{11}Li and ^{11}Be may stem from the magicity loss at $N=8$. Because of deformation, the nuclear systems become more stable and because of the low binding energy of valence neutrons, the orbits become $\ell = 0$ dominant.

The new picture suggests that we have many chances to find out halo nuclei close to the neutron drip-line. Most of nuclei on the nuclear chart are deformed, and valence neutrons may find a low- ℓ dominant Nilsson orbit.

3.3.2 New magicity at $N = 34$

Since magicity loss at $N = 20$ and 28 in the light and neutron-rich nuclei were found, and hence a next question is where large shell gaps exist beyond $N = 28$. A shell model calculation including rather strong monopole residual interactions speculated that $N = 34$ might become a new magic number in the neutron-rich Ca-Ti isotopes [143]. Since then, experimental efforts have been made to access neutron-rich Ca and Ti isotopes and to obtain nuclear properties via mass measurements and gamma spectroscopy. As results, a large shell gap at

$N = 32$ was found in the Ca and Ti isotopes, but no significant gap at $N = 34$ was found in the Ti isotopes. Thus, there was many claims that $N = 34$ might not be magic.

The first spectroscopy of ^{54}Ca was conducted via in-beam gamma spectroscopy at RIBF. Three gamma lines were successfully found [39] and one of them was assigned to be de-excitation gamma ray from 2^+ state to the ground state. According to the systematic trend of 2^+ energy along $Z = 20$ as well as $N = 34$, a large shell gap at $N = 34$ was reduced. At the same time, robustness of $N = 32$ shell gap was also found in ^{50}Ar [50]. Very recently, mass data obtained at SHARAQ suggested the large gap at $N = 34$ [138], too.

The shell gaps at $N = 32$ and 34 correspond to energy differences between $p_{3/2}$ and $p_{1/2}$, and $p_{1/2}$ and $f_{5/2}$, respectively. It is of great interest to find out how the shell gaps would be changed, namely the location of $p_{1/2}$ relative to $p_{3/2}$ and $f_{5/2}$, as a function of Z . In addition, towards the neutron drip-line, the structure study for the neutron-rich Ca isotopes gives hints of three nucleon force effects on the structure. The $Z = 20$ shell gap is large even in the neutron-rich region, thus proton excitation might be frozen and neutron dynamics could be safely studied in the Ca isotopes.

3.3.3 Double magicity of ^{78}Ni

The Ni isotopes with $Z = 28$ magic number are very unique because three neutron magic numbers could be studied with ^{48}Ni , ^{56}Ni and ^{78}Ni . At RIBF, the double magic natures of ^{78}Ni have been focused.

The first spectroscopy data of ^{78}Ni was obtained from systematic half-life measurements around ^{78}Ni [84]. As shown in Fig. 11, observed were sudden changes of half-life between ^{78}Ni and $^{79,80}\text{Ni}$ and also between ^{78}Ni and ^{77}Co . The sudden changes at $Z = 28$ and $N = 50$ may

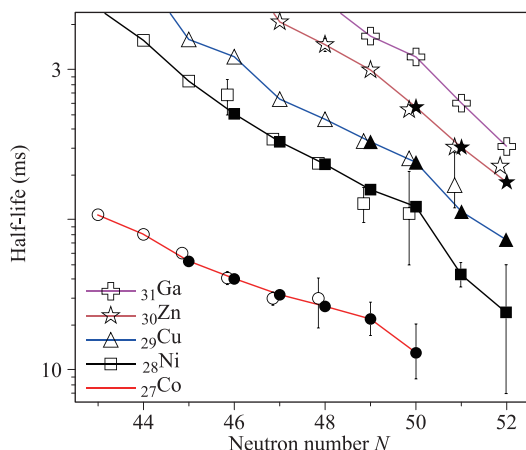


Fig. 11 Half-life of the neutron-rich Co-to-Ga isotopes as a function of N [84].

be caused by sudden changes of β -decay Q value, namely, sudden changes of the nuclear stability. Thus, the observation indicated the double magicity of ^{78}Ni .

In addition to decay spectroscopy, in-beam gamma spectroscopy was conducted to access the ^{78}Ni region. Very recently, one of the results was spectroscopy of ^{79}Cu and discussions were made for the magicity at $Z = 28$ [71].

3.3.4 Magicity at $Z = 50$ or $N = 82$

^{132}Sn is known as a double magic nucleus, of which $Z = 50$ and $N = 82$ shell gaps have been found very large. Thus, the nuclear structure around ^{132}Sn is simply described so far with a model assuming the ^{132}Sn core. With respect of ^{132}Sn , we have accessed at RIBF four regions; “south” ($Z < 50$ and $N = 82$), “south-east” ($Z < 50$ and $N > 82$), “east” ($Z = 50$ and $N > 82$) and “north-east” ($Z > 50$ and $N > 82$), to investigate $Z = 50$ and $N = 82$ shell gaps, proton- and neutron-pairing interactions, and proton-neutron interactions.

In-beam gamma and decay spectroscopy have been employed to observe excited states in the nuclei. The first 2^+ states in even-even nuclei were observed in ^{128}Pd [82] in south, ^{132}Cd [55] in south-east, $^{136,138}\text{Sn}$ [86] in east, and ^{140}Te [111] in north-east. All the data obtained so far indicate large shell gaps at $Z = 50$, and at $N=82$, and no magicity loss has been found.

Among the data introduced above, the ^{132}Cd [55] data was the first spectroscopy data in south-east. It is found that the first excited states in ^{132}Cd and ^{136}Te on the east side are both neutron dominant excited states. On the other hand, concerning the first excited states in ^{128}Cd and ^{132}Te on the west side, contributions of protons to the excited states are almost the same as those of neutrons. It is of great interest that beyond $N = 82$ the neutron matter becomes suddenly soft, and the phenomenon does not depend on the proton number. So far mechanism for the sudden change has not been discussed.

The last topic in this section is a very interesting phenomenon observed in ^{133}Sn [58]. In general, decay of particle unbound states is associated with particle emission and without gamma emission, simply because of coupling constant differences between strong interaction and electro-magnetic interaction. However, we observed gamma decay of an unbound excited state in ^{133}Sn . This might be simply because of small quantum overlap between the excited state in ^{133}Sn and the ground state of ^{132}Sn . This small overlap gives the other evidence that ^{132}Sn has excellent double magicity.

3.4 Impacts on the r -process path

The RIBF is the first facility to give bunch of data associated with the r -process path. According to devel-

opments of astronomical observations and of simulations for supernovae explosion and neutron-star merger, several interesting scenarios have been proposed so far. At present, two scenarios are extensively discussed; cold r -process in neutron-star mergers and hot r -process in supernovae explosions. Due to the recent observation of the gravitational wave from the merger in 2017, the cold r -process attracts much attention in the nuclear physics and astrophysics communities. Data which could be exported from the nuclear physics community are related to nuclear mass, half-life and beta-delayed neutron emission probability. Such information is being provided at RIBF.

The first data produced at RIBF were half-life data for neutron-rich nuclei [76, 89, 109]. The first work was for 38 neutron-rich isotopes in $A \sim 110$ region. The second work covered more neutron-rich nuclei and gave half-lives of 108 neutron-rich isotopes from Rb to Sn. The third one gave half-lives of 94 isotopes from Cs to Ho.

The half-life data obtained are utilized in a network calculation. Figure 12 demonstrates importance of experimental half-life data [89]. The abundance calculation with the new data could reproduce the r -process abundance pattern very well, especially for $A \sim 120$ region and $A \sim 140\text{--}160$ region. The third data set [109] has striking, large drops of half-lives at $N = 97$ for Ce, Pr, Nd and Sm and $N = 105$ for Eu, Gd, Tb and Dy, and has a direct impact in the r -process abundance calculations affecting almost all mass numbers between $A = 150$ and 170.

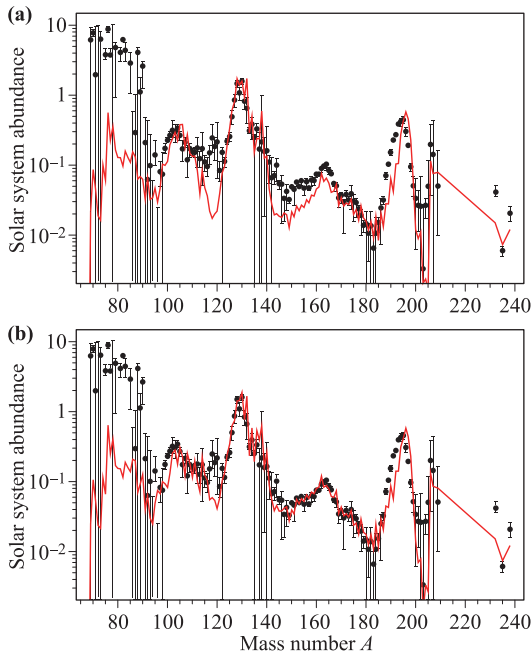


Fig. 12 Comparison between the r -process abundance pattern and abundances calculated (a) without and (b) with new half-life data [89].

Coming data for the neutron-emission probability and mass information should give further impacts of data to the r -process path study.

3.5 Nucleon correlation

Due to the recent potentials of gravitational wave observations, equation-of-state in asymmetric nuclear matter has attracted much attention. There are many approaches to get EOS information, and here microscopic few-body interaction studies at RIBF are introduced.

To understand the structure of neutron-stars, we need EOS over a wide dynamic range of density. When the density is increased, many-body forces such as three nucleon force (3NF) become important. Nowadays, effect of 3NF to the nuclear structure is one of the major subjects for theoretical and experimental works. At RIBF, polarized deuteron + proton elastic scattering has been studied to obtain $T = 1/2$ channel of 3NF. The energy dependences and deuteron analyzing power dependences have been given to construct fundamental interaction sets for ab-initio calculations [19–21].

An experimental attempt was made to observe resonant four neutron state, “tetra” neutron state with missing mass spectroscopy [135]. The reported result is very exciting, which shows a candidate of the state at ~ 1 MeV above the threshold, as shown in Fig. 13. The data is very useful to investigate many-body forces such as $T = 3/2$ and $T = 2$ channels. Very recently, the study was re-visited to have more statistics data. The tetra neutron work has made a great trigger to investigate very

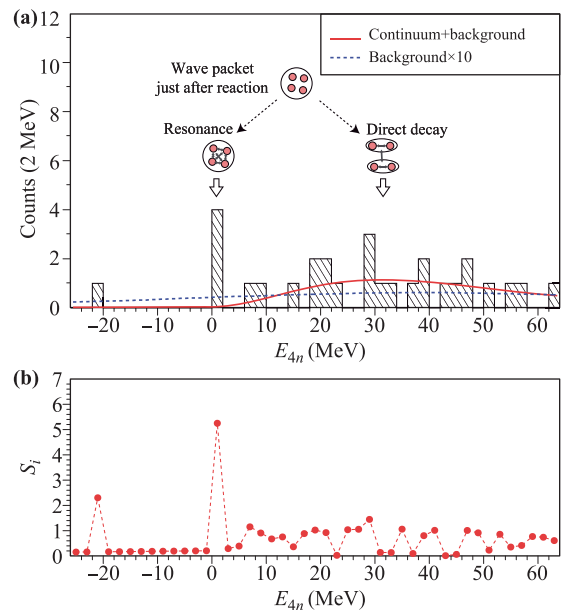


Fig. 13 (a) Missing-mass spectrum of the tetra neutron system. (b) Evaluation of the goodness of fit [135].

exotic few-body systems such as ${}^7\text{H}$. The data obtained at SAMURAI are now under analysis.

3.6 Reaction study with long-lived fission products in nuclear wastes

Reduction of high-level radioactive waste is one of the major goals of sustainable development for society. Research and development into the reduction using partitioning and transmutation (P & T) technology have been conducted over recent decades in the world.

At RIBF, based on intense RI beams, reaction study with long-lived fission products such as ${}^{137}\text{Cs}$, ${}^{90}\text{Sr}$, ${}^{107}\text{Pd}$ and ${}^{90}\text{Zr}$ was organized for nuclear transmutation [126–128]. So called “inverse kinematics” technique was employed to obtain spallation reaction data. The advantage of the inverse kinematics technique gives clear particle identification for reaction products and gives easy control of RI beam energies for energy-dependence study, thus nice quality of the data was achieved at RIBF. Proton- and deuteron-induced reactions were systematically studied, and these data are very useful to improve reaction theories and simulation tools.

4 Summary and outlook

Since RIBF started operation in 2007, multitudes of data have been published for a variety of subjects in nuclear physics. The high productivity of RIBF is based on stable operations of RIBF realized by year-by-year upgrade of the accelerator complex and of experimental devices.

The potentials of RIBF have been demonstrated with more than 130 new isotopes made. Thanks to intense and fast RI beams available, not only decay spectroscopy but also reaction study to obtain nuclear properties of exotic nuclei have been made. Concerning the shell evolution, the ground state properties of both neutron-rich and neutron-deficient nuclei have been obtained in a wide region of $A \sim 20$ –160, and magicity loss at $N = 28$, new magicity at $N = 34$, and robustness of magicity $N = 50$ up to $Z = 28$, and of $N = 82$ up to $Z = 46$ have been found. The bunch of half-life data have been produced for the r -process path, which show the importance of experimental data in the r -process discussion. Nucleon correlation study has been in progress to create very exotic light and neutron-rich nuclear systems. The new project associated with the nuclear transmutation was launched for the nuclear waste problem.

Although many findings are being produced, we need more experimental data to test theoretical models, to encourage theorists to give more accurate predictions for nuclear properties. Data of the beta-delayed neutron emission probability will come out soon. Nuclear moment data will be provided based on the novel technique

of spin-aligned RI beams. Nuclear mass data and charge form factor data will be produced at the R^3 and SCRIT system, respectively.

Concerning a long-range perspective for trends of nuclear physics, three directions are being discussed; higher excitation energy, heavier nuclei, and EOS. So far discussions of shell evolution are limited to the ground state properties. When we move to high excited states, a variety of collective modes based on a variety of symmetry are predicted to emerge. An interesting topic is how cluster states would be developed in neutron-rich nuclei. To understand fission dynamics, we need to know the shell structure at finite temperature. In heavy nuclei, a key ingredient is Coulomb force effects to the nuclear structure. One alpha separation energy is going to be negative in the heavy mass region. This suggests that cluster formation or cluster effects could be studied rather easily. The gravitation wave observations in this Century give unique opportunities to test EOS made by microscopic interactions and also by many-body force effects. The gravitation waves would connect a tiny object of nuclei and a big object of neutron stars.

Acknowledgements Prof. Akito Arima was the President of RIKEN from October 1993 to May 1998, and during the period, Prof. Arima supported the “Radioactive Isotope Beam Factory” (RIBF) project and gave us an ignition key to start the project. At this special occasion of Prof. Akito Arima’s 88th birthday anniversary, this paper is dedicated to him due to his great support and encouragement for RIBF.

References

1. Y. Yano, The RIKEN RI Beam Factory Project: A status report, *Nucl. Instrum. Methods Phys. Res. Sect. B* 261(1–2), 1009 (2007)
2. T. Kubo, M. Ishihara, N. Inabe, H. Kumagai, I. Tanihata, et al., The RIKEN radioactive beam facility, *Nucl. Instrum. Methods Phys. Res. Sect. B* 70(1–4), 309 (1992)
3. K. Morita, K. Morimoto, D. Kaji, T. Akiyama, S. Goto, et al., Experiment on the synthesis of element 113 in the reaction ${}^{209}\text{Bi}({}^{70}\text{Zn},n){}^{278}113$, *JPSJ* 73(10), 2593 (2004)
4. K. Morita, K. Morimoto, D. Kaji, T. Akiyama, S. Goto, et al., Observation of second decay chain from ${}^{278}113$, *JPSJ* 76(4), 045001 (2007)
5. K. Morita, K. Morimoto, D. Kaji, H. Haba, K. Ozeki, et al., New result in the production and decay of an isotope, ${}^{278}113$, of the 113th element, *JPSJ* 81(10), 103201 (2012)
6. H. Okuno, N. Fukunishi, and O. Kamigaito, Progress of RIBF accelerators, *Prog. Theor. Exp. Phys.* 2012, 03C002 (2012)
7. T. Kubo, D. Kameda, H. Suzuki, N. Fukuda, H. Takeda, et al., BigRIPS separator and ZeroDegree spectrometer

- at RIKEN RI Beam Factory, *Prog. Theor. Exp. Phys.* 2012, 03C003 (2012)
8. T. Ohnishi, T. Kubo, K. Kusaka, A. Yoshida, K. Yoshida, et al., Identification of new isotopes ^{125}Pd and ^{126}Pd produced by in-flight fission of 345 MeV/nucleon ^{238}U : First results from the RIKEN RI Beam Factory, *J. Phys. Soc. Jpn.* 77(8), 083201 (2008)
 9. T. Motobayashi and H. Sakurai, Research with fast radioactive isotope beams at RIKEN, *Prog. Theor. Exp. Phys.* 2012, 03C001 (2012)
 10. S. Kubono, Y. Yanagisawa, T. Teranishi, et al., New low-energy RIB separator CRIB for nuclear astrophysics, *Eur. Phys. J. A* 13, 217 (2002)
 11. Y. Hirayama, Y. Watanabe, N. Imai, et al., Off-line test of the KISS gas cell, *Nucl. Instrum. Methods Phys. Res. Sect. B* 317, 480 (2013)
 12. T. Nakamura, H. Sakurai, and H. Watanabe, Exotic nuclei explored at in-flight separators, *Prog. Part. Nucl. Phys.* 97, 53 (2017)
 13. T. Kobayashi, N. Chiga, T. Isobe, Y. Kondo, T. Kubo, et al., SAMURAI spectrometer for RI beam experiments, *Nucl. Instrum. Methods Phys. Res. Sect. B* 317, 294 (2013)
 14. T. Uesaka, et al. (SHARAQ Collaboration), The SHARAQ spectrometer, *Prog. Theor. Exp. Phys.* 2012, 03C007 (2012)
 15. A. Ozawa, T. Uesaka, and M. Wakasugi, The rare-RI ring, *Prog. Theor. Exp. Phys.* 2012, 03C009 (2012)
 16. M. Wakasugi, T. Emoto, S. Ito, S. Wang, T. Suda, Y. Yano, K. Kurita, K. Ishii, T. Tamae, A. Kuwajima, A. Noda, T. Shiari, and H. Tongu, Electron scattering based on a novel internal target technique: SCRIT, *Eur. Phys. J. A* 42(3), 453 (2009)
 17. T. Suda, et al., Nuclear physics at the SCRIT electron scattering facility, *Prog. Theor. Exp. Phys.* 2012, 03C008 (2012)
 18. M. Wada, Genealogy of gas cells for low-energy RI-beam production, *Nucl. Instrum. Methods Phys. Res. Sect. B* 317, 450 (2013)
 19. K. Sekiguchi, H. Okamura, N. Sakamoto, H. Suzuki, M. Dozono, et al., Three nucleon force effects in intermediate-energy deuteron analyzing powers for dp elastic scattering, *Phys. Rev. C* 83(6), 061001 (2011)
 20. K. Sekiguchi, Y. Wada, J. Miyazaki, H. Witala, M. Dozono, et al., Complete set of deuteron analyzing powers for dp elastic scattering at 250–294 MeV/nucleon and the three-nucleon force, *Phys. Rev. C* 89(6), 064007 (2014)
 21. K. Sekiguchi, H. Witala, T. Akieda, D. Eto, H. Kon, et al., Complete set of deuteron analyzing powers from \vec{dp} elastic scattering at 190 MeV/nucleon, *Phys. Rev. C* 96(6), 064001 (2017)
 22. T. Ohnishi, T. Kubo, K. Kusaka, A. Yoshida, K. Yoshida, et al., Identification of 45 new neutron-rich isotopes produced by in-flight fission of a ^{238}U Beam at 345 MeV/nucleon, *J. Phys. Soc. Jpn.* 79(7), 073201 (2010)
 23. N. Fukuda, T. Kubo, D. Kameda, N. Inabe, H. Suzuki, et al., Identification of new neutron-rich isotopes in the rare-earth region produced by 345 MeV/nucleon ^{238}U , *J. Phys. Soc. Jpn.* 87(1), 014202 (2018)
 24. H. Suzuki, T. Kubo, N. Fukuda, N. Inabe, D. Kameda, et al., Discovery of new isotopes $^{81,82}\text{Mo}$ and $^{85,86}\text{Ru}$ and a determination of the particle instability of ^{103}Sb , *Phys. Rev. C* 96(3), 034604 (2017)
 25. O. B. Tarasov, D. S. Ahn, D. Bazin, N. Fukuda, A. Gade, et al., Discovery of ^{60}Ca and implications for the stability of ^{70}Ca , *Phys. Rev. Lett.* 121(2), 022501 (2018)
 26. D. Kameda, T. Kubo, T. Ohnishi, K. Kusaka, A. Yoshida, et al., Observation of new microsecond isomers among fission products from in-flight fission of 345 MeV/nucleon ^{238}U , *Phys. Rev. C* 86(5), 054319 (2012)
 27. M. Takechi, T. Ohtsubo, M. Fukuda, D. Nishimura, T. Kuboki, et al., Interaction cross sections for Ne isotopes towards the island of inversion and halo structures of ^{29}Ne and ^{31}Ne , *Phys. Lett. B* 707(3–4), 357 (2012)
 28. M. Takechi, S. Suzuki, D. Nishimura, M. Fukuda, T. Ohtsubo, et al., Evidence of halo structure in ^{37}Mg observed via reaction cross sections and intruder orbitals beyond the island of inversion, *Phys. Rev. C* 90(6), 061305 (2014) (R)
 29. Y. Ichikawa, H. Ueno, Y. Ishii, T. Furukawa, A. Yoshimi, et al., Production of spin-controlled rare isotope beams, *Nat. Phys.* 8(12), 918 (2012)
 30. T. Nishi, K. Itahashi, G. P. A. Berg, H. Fujioka, N. Fukuda, et al., Spectroscopy of pionic atoms in $^{122}\text{Sn}(d, ^3\text{He})$ reaction and angular dependence of the formation cross sections, *Phys. Rev. Lett.* 120(15), 152505 (2018)
 31. P. Doornenbal, In-beam gamma-ray spectroscopy at the RIBF, *Prog. Theor. Exp. Phys.* 2012, 03C004 (2012)
 32. S. Takeuchi, T. Motobayashi, Y. Togano, et al., DALI2: A NaI(Tl) detector array for measurements of γ rays from fast nuclei, *Nucl. Instrum. Methods Phys. Res. Sect. A* 763, 596 (2014)
 33. P. Doornenbal, H. Scheit, N. Aoi, S. Takeuchi, K. Li, et al., Spectroscopy of Ne 32 and the “Island of Inversion”, *Phys. Rev. Lett.* 103(3), 032501 (2009)
 34. T. Nakamura, N. Kobayashi, Y. Kondo, Y. Satou, N. Aoi, et al., Halo Structure of the Island of Inversion Nucleus Ne 31, *Phys. Rev. Lett.* 103(26), 262501 (2009)
 35. P. Doornenbal, H. Scheit, N. Kobayashi, N. Aoi, S. Takeuchi, et al., Exploring the “island of inversion” by in-beam γ -ray spectroscopy of the neutron-rich sodium isotopes $^{31,32,33}\text{Na}$, *Phys. Rev. C* 81(4), 041305 (2010)

36. K. A. Li, Y. L. Ye, H. Scheit, P. Doornenbal, T. Satoshi, A. Nori, M. Masafumi, T. Eri, M. Tohr, S. Hiro Yoshi, and D.Y. Pang, Inelastic scattering of ^{32}Mg at 190 MeV/nucleon from a thick proton target, *Chin. Phys. Lett.* 29(10), 102301 (2012)
37. S. Takeuchi, M. Matsushita, N. Aoi, P. Doornenbal, K. Li, et al., Well developed deformation in ^{42}Si , *Phys. Rev. Lett.* 109(18), 182501 (2012)
38. N. Kobayashi, T. Nakamura, J. A. Tostevin, Y. Kondo, N. Aoi, et al., One- and two-neutron removal reactions from the most neutron-rich carbon isotopes, *Phys. Rev. C* 86(5), 054604 (2012)
39. D. Steppenbeck, S. Takeuchi, N. Aoi, P. Doornenbal, M. Matsushita, et al., Evidence for a new nuclear “magic number” from the level structure of ^{54}Ca , *Nature* 502(7470), 207 (2013)
40. L. Audirac, A. Obertelli, P. Doornenbal, D. Mancusi, S. Takeuchi, et al., Evaporation-cost dependence in heavy-ion fragmentation, *Phys. Rev. C* 88(4), 041602 (2013)
41. P. Doornenbal, H. Scheit, S. Takeuchi, N. Aoi, K. Li, et al., In-beam γ -ray spectroscopy of $^{34,36,38}\text{Mg}$: Merging the $N = 20$ and $N = 28$ shell quenching, *Phys. Rev. Lett.* 111(21), 212502 (2013)
42. H. Wang, N. Aoi, S. Takeuchi, M. Matsushita, P. Doornenbal, et al., Collectivity evolution in the neutron-rich Pd isotopes toward the $N = 82$ shell closure, *Phys. Rev. C* 88(5), 054318 (2013)
43. H. Wang, N. Aoi, S. Takeuchi, et al., Structure of ^{136}Sn and the $Z = 50$ magicity, *Prog. Theor. Exp. Phys.* 2014, 023D02 (2014)
44. T. Nakamura, N. Kobayashi, Y. Kondo, Y. Satou, J. A. Tostevin, et al., Deformation-Driven p-Wave Halos at the Drip Line: Ne 31, *Phys. Rev. Lett.* 112(14), 142501 (2014)
45. H. L. Crawford, P. Fallon, A. O. Macchiavelli, R. M. Clark, B. A. Brown, et al., Shell and shape evolution at $N = 28$: The ^{40}Mg ground state, *Phys. Rev. C* 89(4), 041303 (2014)
46. P. Doornenbal, H. Scheit, S. Takeuchi, et al., Rotational level structure of sodium isotopes inside the “island of inversion”, *Prog. Theor. Exp. Phys.* 2014, 053D01 (2014)
47. N. Kobayashi, T. Nakamura, Y. Kondo, J. A. Tostevin, Y. Utsuno, et al., Observation of a p-wave one-neutron halo configuration in ^{37}Mg , *Phys. Rev. Lett.* 112(24), 242501 (2014)
48. P. Doornenbal, S. Takeuchi, N. Aoi, M. Matsushita, A. Obertelli, et al., Intermediate-energy Coulomb excitation of ^{104}Sn : Moderate $E2$ strength decrease approaching ^{100}Sn , *Phys. Rev. C* 90(6), 061302 (2014)
49. A. Corsi, S. Boissinot, A. Obertelli, P. Doornenbal, M. Dupuis, et al., Neutron-driven collectivity in light tin isotopes: Proton inelastic scattering from ^{104}Sn , *Phys. Lett. B* 743, 451 (2015)
50. D. Steppenbeck, S. Takeuchi, N. Aoi, P. Doornenbal, M. Matsushita, et al., Low-lying structure of ^{50}Ar and the $N = 32$ subshell closure, *Phys. Rev. Lett.* 114(25), 252501 (2015)
51. K. Li, Y. Ye, T. Motobayashi, H. Scheit, P. Doornenbal, S. Takeuchi, N. Aoi, M. Matsushita, E. Takeshita, D. Pang, and H. Sakurai, Relativistic Coulomb excitation in ^{32}Mg near 200 MeV/nucleon with a thick target, *Phys. Rev. C* 92(1), 014608 (2015)
52. N. Kobayashi, T. Nakamura, Y. Kondo, J. A. Tostevin, N. Aoi, et al., One-neutron removal from ^{29}Ne : Defining the lower limits of the island of inversion, *Phys. Rev. C* 93(1), 014613 (2016)
53. Y. Shiga, K. Yoneda, D. Steppenbeck, N. Aoi, P. Doornenbal, et al., Investigating nuclear shell structure in the vicinity of ^{78}Ni : Low-lying excited states in the neutron-rich isotopes $^{80,82}\text{Zn}$, *Phys. Rev. C* 93(2), 024320 (2016)
54. P. Doornenbal, H. Scheit, S. Takeuchi, N. Aoi, K. Li, et al., Mapping the deformation in the “island of inversion”: Inelastic scattering of ^{30}Ne and ^{36}Mg at intermediate energies, *Phys. Rev. C* 93(4), 044306 (2016)
55. H. Wang, N. Aoi, S. Takeuchi, M. Matsushita, T. Motobayashi, et al., First spectroscopic information from even-even nuclei in the region “southeast” of ^{132}Sn : Neutron-excitation dominance of the $21+$ state in ^{132}Cd , *Phys. Rev. C* 94(5), 051301 (2016)
56. H. N. Liu, J. Lee, P. Doornenbal, H. Scheit, S. Takeuchi, et al., Intruder configurations in the ground state of ^{30}Ne , *Phys. Lett. B* 767, 58 (2017)
57. N. Nakatsuka, H. Baba, T. Aumann, R. Avigo, S. R. Banerjee, et al., Observation of isoscalar and isovector dipole excitations in neutron-rich ^{20}O , *Phys. Lett. B* 768, 387 (2017)
58. V. Vaquero, A. Jungclaus, P. Doornenbal, K. Wimmer, A. Gargano, et al., Gamma decay of unbound neutron-hole states in ^{133}Sn , *Phys. Rev. Lett.* 118(20), 202502 (2017)
59. P. Doornenbal, H. Scheit, S. Takeuchi, Y. Utsuno, N. Aoi, et al., Low- Z shore of the “island of inversion” and the reduced neutron magicity toward ^{28}O , *Phys. Rev. C* 95(4), 041301 (2017)
60. S. Momiyama, P. Doornenbal, H. Scheit, S. Takeuchi, M. Niikura, et al., In-beam γ -ray spectroscopy of ^{35}Mg via knockout reactions at intermediate energies, *Phys. Rev. C* 96(3), 034328 (2017)
61. A. Corsi, A. Obertelli, P. Doornenbal, F. Nowacki, H. Sagawa, et al., Spectroscopy of nuclei around ^{100}Sn populated via two-neutron knockout reactions, *Phys. Rev. C* 97(4), 044321 (2018)
62. Zs. Vajta, D. Sohler, Y. Shiga, K. Yoneda, K. Sieja, et al., Proton single particle energies next to ^{78}Ni : Spectroscopy of ^{77}Cu via single proton knock-out reaction, *Phys. Lett. B* 782, 99 (2018)

63. H. Wang, N. Aoi, S. Takeuchi, M. Matsushita, P. Doornenbal, T. Motobayashi, D. Steppenbeck, K. Yoneda, K. Kobayashi, J. Lee, H.N. Liu, Y. Kondo, R. Yokoyama, H. Sakurai, and Y.L. Ye, Observation of new isotope ^{131}Ag via the two-step fragmentation technique, *Chin. Phys. Lett.* 30(4), 042501 (2013)
64. A. Obertelli, A. Delbart, S. Anvar, L. Audirac, G. Authélet, et al., MINOS: A vertex tracker coupled to a thick liquid-hydrogen target for in-beam spectroscopy of exotic nuclei, *Eur. Phys. J. A* 50(1), 8 (2014)
65. C. Santamaria, C. Louchart, A. Obertelli, V. Werner, P. Doornenbal, et al., Extension of the $N = 40$ island of inversion towards $N = 50$: Spectroscopy of ^{66}Cr , $^{70,72}\text{Fe}$, *Phys. Rev. Lett.* 115(19), 192501 (2015)
66. N. Paul, A. Corsi, A. Obertelli, P. Doornenbal, G. Authélet, et al., Are there signatures of harmonic oscillator shells far from stability? First spectroscopy of ^{110}Zr , *Phys. Rev. Lett.* 118(3), 032501 (2017)
67. F. Flavigny, P. Doornenbal, A. Obertelli, J. P. Delaroche, M. Girod, et al., Shape evolution in neutron-rich krypton isotopes beyond $N = 60$: First spectroscopy of $^{98,100}\text{Kr}$, *Phys. Rev. Lett.* 118(24), 242501 (2017)
68. S. Chen, P. Doornenbal, A. Obertelli, T. R. Rodríguez, G. Authélet, et al., Low-lying structure and shape evolution in neutron-rich Se isotopes, *Phys. Rev. C* 95(4), 041302 (2017)
69. M. Lettmann, V. Werner, N. Pietralla, P. Doornenbal, A. Obertelli, et al., Triaxiality of neutron-rich $^{84,86,88}\text{Ge}$ from low-energy nuclear spectra, *Phys. Rev. C* 96(1), 011301 (2017)
70. C. M. Shand, Zs. Podolyak, M. Gorska, P. Doornenbal, A. Obertelli, et al., Shell evolution beyond $Z = 28$ and $N = 50$: Spectroscopy of $^{81,82,83,84}\text{Zn}$, *Phys. Lett. B* 773, 492 (2017)
71. L. Olivier, S. Franchoo, M. Niikura, Z. Vajta, D. Sohler, et al., Persistence of the $Z = 28$ shell gap around ^{78}Ni : First spectroscopy of ^{79}Cu , *Phys. Rev. Lett.* 119(19), 192501 (2017)
72. M. L. Cortés, P. Doornenbal, M. Dupuis, S. M. Lenzi, F. Nowacki, et al., Inelastic scattering of neutron-rich Ni and Zn isotopes off a proton target, *Phys. Rev. C* 97(4), 044315 (2018)
73. E. Pollacco, D. Beaumel, P. Roussel-Chomaz, E. Atkin, P. Baron, et al., MUST2: A new generation array for direct reaction studies, *Eur. Phys. J. A* 25(S1), 287 (2005)
74. V. Lapoux, S. Boissinot, H. Otsu, H. Baba, R. J. Chen, et al., Spectroscopy of the unbound states of the drip-line nucleus ^{24}O , *Prog. Theor. Phys. Suppl.* 196, 111 (2012)
75. S. Nishimura, et al., Beta-gamma spectroscopy at RIBF, *Prog. Theor. Exp. Phys.* 2012, 03C006 (2012)
76. S. Nishimura, Z. Li, H. Watanabe, K. Yoshinaga, T. Sumikama, et al., β -decay half-lives of very neutron-rich Kr to Tc isotopes on the boundary of the r -process path: An indication of fast r -matter flow, *Phys. Rev. Lett.* 106(5), 052502 (2011)
77. H. Watanabe, T. Sumikama, S. Nishimura, K. Yoshinaga, Z. Li, et al., Low-lying level structure of the neutron-rich nucleus ^{109}Nb : A possible oblate-shape isomer, *Phys. Lett. B* 696(3), 186 (2011)
78. T. Sumikama, K. Yoshinaga, H. Watanabe, S. Nishimura, Y. Miyashita, et al., Structural evolution in the neutron-rich nuclei ^{106}Zr and ^{108}Zr , *Phys. Rev. Lett.* 106(20), 202501 (2011)
79. H. Watanabe, K. Yamaguchi, A. Odahara, T. Sumikama, S. Nishimura, et al., Development of axial asymmetry in the neutron-rich nucleus ^{110}Mo , *Phys. Lett. B* 704(4), 270 (2011)
80. P.A. Soderstrom, S. Nishimura, P. Doornenbal, G. Lorusso, T. Sumikama, et al., Installation and commissioning of EURICA – Euroball-RIKEN cluster array, *Nucl. Instrum. Methods Phys. Res. Sect. B* 317, 649 (2013)
81. P. A. Söderström, G. Lorusso, H. Watanabe, S. Nishimura, P. Doornenbal, et al., Shape evolution in $^{116,118}\text{Ru}$: Triaxiality and transition between the O(6) and U(5) dynamical symmetries, *Phys. Rev. C* 88(2), 024301 (2013)
82. H. Watanabe, G. Lorusso, S. Nishimura, Z. Y. Xu, T. Sumikama, et al., Isomers in ^{128}Pd and ^{126}Pd : Evidence for a robust shell closure at the neutron magic number 82 in exotic palladium isotopes, *Phys. Rev. Lett.* 111(15), 152501 (2013)
83. J. Taprogge, A. Jungclaus, H. Grawe, S. Nishimura, P. Doornenbal, et al., $1p_{3/2}$ proton-hole state in ^{132}Sn and the shell structure along $N = 82$, *Phys. Rev. Lett.* 112(13), 132501 (2014)
84. Z. Y. Xu, S. Nishimura, G. Lorusso, F. Browne, P. Doornenbal, et al., β -decay half-lives of $^{76,77}\text{Co}$, $^{79,80}\text{Ni}$, and ^{81}Cu : Experimental indication of a doubly magic ^{78}Ni , *Phys. Rev. Lett.* 113(3), 032505 (2014)
85. H. Watanabe, G. Lorusso, S. Nishimura, T. Otsuka, K. Ogawa, et al., Monopole-driven shell evolution below the doubly magic nucleus ^{132}Sn explored with the long-lived isomer in ^{126}Pd , *Phys. Rev. Lett.* 113(4), 042502 (2014)
86. G. S. Simpson, G. Gey, A. Jungclaus, J. Taprogge, S. Nishimura, et al., Yrast 6^+ seniority isomers of $^{136,138}\text{Sn}$, *Phys. Rev. Lett.* 113(13), 132502 (2014)
87. J. Taprogge, A. Jungclaus, H. Grawe, S. Nishimura, Z. Y. Xu, et al., Identification of a millisecond isomeric state in $^{129}\text{Cd}_{81}$ via the detection of internal conversion and Compton electrons, *Phys. Lett. B* 738, 223 (2014)
88. Z. Patel, P.A. Söderström, Z. Podolyák, P. H. Regan, P. M. Walker, et al., Isomer decay spectroscopy of ^{164}Sm and ^{166}Gd : Midshell collectivity around $N = 100$, *Phys. Rev. Lett.* 113(26), 262502 (2014)
89. G. Lorusso, S. Nishimura, Z. Y. Xu, A. Jungclaus, Y. Shimizu, et al., β -decay half-lives of 110 neutron-rich nuclei across the $N = 82$ shell gap: Implications for the mechanism and universality of the astrophysical r process, *Phys. Rev. Lett.* 114(19), 192501 (2015)

90. J. Taprogge, A. Jungclaus, H. Grawe, S. Nishimura, P. Doornenbal, et al., β decay of ^{129}Cd and excited states in ^{129}In , *Phys. Rev. C* 91(5), 054324 (2015)
91. R. Lozeva, A. Odahara, C. B. Moon, et al., New decay scheme of the $^{136}_{51}\text{Sb}_{85}$ 6^- isomer, *Phys. Rev. C* 92, 024304 (2015)
92. F. Browne, A. M. Bruce, T. Sumikama, I. Nishizuka, S. Nishimura, et al., Lifetime measurements of the first 2^+ states in $^{104,106}\text{Zr}$: Evolution of ground-state deformations, *Phys. Lett. B* 750, 448 (2015)
93. G. Benzoni, A. I. Morales, H. Watanabe, S. Nishimura, L. Coraggio, et al., Decay properties of $^{68,69,70}\text{Mn}$: Probing collectivity up to $N = 44$ in Fe isotopic chain, *Phys. Lett. B* 751, 107 (2015)
94. P. Lee, C. B. Moon, C. S. Lee, A. Odahara, R. Lozeva, et al., β -delayed γ -ray spectroscopy of non-yrast states in ^{138}Te near the neutron drip line, *Phys. Rev. C* 92(4), 044320 (2015)
95. P. A. Söderström, S. Nishimura, Z. Y. Xu, K. Sieja, V. Werner, et al., Two-hole structure outside ^{78}Ni : Existence of a m s isomer of ^{76}Co and b decay into ^{76}Ni , *Phys. Rev. C* 92(5), 051305 (2015) (R)
96. Z. Patel, Z. Podolyák, P. M. Walker, P. H. Regan, P. A. Söderström, et al., Decay spectroscopy of ^{160}Sm : The lightest four-quasiparticle K isomer, *Phys. Lett. B* 753, 182 (2016)
97. R. Lozeva, H. Naidja, F. Nowacki, J. Dudek, A. Odahara, et al., New isomer found in $^{140}_{51}\text{Sb}_{89}$: Sphericity and shell evolution between $N = 82$ and $N = 90$, *Phys. Rev. C* 93(1), 014316 (2016)
98. A. I. Morales, G. Benzoni, H. Watanabe, S. Nishimura, F. Browne, et al., Low-lying excitations in ^{72}Ni , *Phys. Rev. C* 93(3), 034328 (2016)
99. A. Jungclaus, A. Gargano, H. Grawe, J. Taprogge, S. Nishimura, et al., First observation of γ rays emitted from excited states south-east of ^{132}Sn : The $\pi g_{9/2}^{-1} \otimes \nu f_{7/2}$ multiplet of $^{132}\text{In}_{83}$, *Phys. Rev. C* 93(4), 041301 (2016) (R)
100. I. Čeliković, M. Lewitowicz, R. Gernhauser, R. Krücken, S. Nishimura, et al., New isotopes and proton emitters—crossing the drip line in the vicinity of ^{100}Sn , *Phys. Rev. Lett.* 116(16), 162501 (2016)
101. B. Blank, T. Goigoux, P. Ascher, M. Gerbaux, J. Giovinazzo, et al., New neutron-deficient isotopes from ^{78}Kr fragmentation, *Phys. Rev. C* 93(6), 061301 (2016) (R)
102. H. Watanabe, G. X. Zhang, K. Yoshida, P. M. Walker, J. J. Liu, et al., Long-lived K isomer and enhanced γ vibration in the neutron-rich nucleus ^{172}Dy : Collectivity beyond double midshell, *Phys. Lett. B* 760, 641 (2016)
103. A. Jungclaus, H. Grawe, S. Nishimura, P. Doornenbal, G. Lorusso, et al., β decay of semi-magic ^{130}Cd : Revision and extension of the level scheme of ^{130}In , *Phys. Rev. C* 94(2), 024303 (2016)
104. T. Goigoux, P. Ascher, B. Blank, M. Gerbaux, J. Giovinazzo, et al., Two-proton radioactivity of ^{67}Kr , *Phys. Rev. Lett.* 117(16), 162501 (2016)
105. P. A. Söderström, P. M. Walker, J. Wu, H. L. Liu, P. H. Regan, et al., K-mixing in the doubly mid-shell nuclide ^{170}Dy and the role of vibrational degeneracy, *Phys. Lett. B* 762, 404 (2016)
106. J. Taprogge, A. Jungclaus, H. Grawe, I. N. Borzov, S. Nishimura, et al., Proton-hole and core-excited states in the semi-magic nucleus $^{131}\text{In}_{82}$, *Eur. Phys. J. A* 52(11), 347 (2016)
107. E. Ideguchi, G. S. Simpson, R. Yokoyama, M. Tanaka, S. Nishimura, et al., ms isomers of $^{158,160}\text{Nd}$, *Phys. Rev. C* 94(6), 064322 (2016)
108. A. I. Morales, G. Benzoni, H. Watanabe, Y. Tsunoda, T. Otsuka, et al., Type II shell evolution in $A = 70$ isobars from the $N \geq 40$ island of inversion, *Phys. Lett. B* 765, 328 (2017)
109. J. Wu, S. Nishimura, G. Lorusso, P. Möller, E. Ideguchi, et al., 94 β -decay half-lives of neutron-rich $_{55}\text{Cs}$ to $_{67}\text{Ho}$: Experimental feedback and evaluation of the r -process rare-earth peak formation, *Phys. Rev. Lett.* 118(7), 072701 (2017)
110. P. J. Davies, H. Grawe, K. Moschner, A. Blazhev, R. Wadsworth, et al., The role of core excitations in the structure and decay of the 16^+ spin-gap isomer in ^{96}Cd , *Phys. Lett. B* 767, 474 (2017)
111. B. Moon, C. B. Moon, P. A. Soderstrom, A. Odahara, R. Lozeva, et al., Nuclear structure and β -decay schemes for Te nuclides beyond $N = 82$, *Phys. Rev. C* 95(4), 044322 (2017)
112. T. Sumikama, S. Nishimura, H. Baba, F. Browne, P. Doornenbal, et al., Observation of new neutron-rich Mn, Fe, Co, Ni, and Cu isotopes in the vicinity of ^{78}Ni , *Phys. Rev. C* 95(5), 051601 (2017) (R)
113. E. Sahin, F. L. Bello Garrote, Y. Tsunoda, T. Otsuka, G. de Angelis, et al., Shell evolution towards ^{78}Ni : Low-lying states in ^{77}Cu , *Phys. Rev. Lett.* 118(24), 242502 (2017)
114. A. I. Morales, A. Algora, B. Rubio, K. Kaneko, S. Nishimura, et al., Simultaneous investigation of the $T = 1$ ($J^\pi = 0^+$) and $T = 0$ ($J^\pi = 9^+$) β decays in ^{70}Br , *Phys. Rev. C* 95(6), 064327 (2017)
115. A. Jungclaus, H. Grawe, S. Nishimura, P. Doornenbal, G. Lorusso, et al., Observation of a γ -decaying millisecond isomeric state in $^{128}\text{Cd}_{80}$, *Phys. Lett. B* 772, 483 (2017)
116. B. Moon, C. B. Moon, A. Odahara, R. Lozeva, P. A. Söderström, et al., b-decay scheme of ^{140}Te to ^{140}I : Suppression of Gamow–Teller transitions between the neutron $h_{9/2}$ and proton $h_{11/2}$ partner orbitals, *Phys. Rev. C* 96(1), 014325 (2017)
117. F. Browne, A. M. Bruce, T. Sumikama, I. Nishizuka, S. Nishimura, et al., K selection in the decay of the $(\nu 5/2 [32] \otimes 3/2 [411])$ 4^- isomeric state in ^{102}Zr , *Phys. Rev. C* 96(2), 024309 (2017)

118. Z. Patel, P. M. Walker, Zs. Podolyak, P. H. Regan, T. A. Berry, et al., Isomer-delayed γ -ray spectroscopy of $A = 159$ – 164 midshell nuclei and the variation of K-forbidden $E1$ transition hindrance factors, *Phys. Rev. C* 96(3), 034305 (2017)
119. J. Park, R. Krucken, D. Lubos, R. Gernhäuser, M. Lewitowicz, et al., Properties of γ -decaying isomers and isomeric ratios in the ^{100}Sn region, *Phys. Rev. C* 96(4), 044311 (2017)
120. H. Suzuki, L. Sinclair, P. A. Soderstrom, G. Lorusso, P. Davies, et al., Discovery of ^{72}Rb : A nuclear sandbank beyond the proton drip line, *Phys. Rev. Lett.* 119(19), 192503 (2017)
121. Y. Shimizu, T. Kubo, N. Fukuda, N. Inabe, D. Kameda, et al., Observation of New Neutron-rich Isotopes among Fission Fragments from In-flight Fission of 345 MeV/nucleon ^{238}U : Search for New Isotopes Conducted Concurrently with Decay Measurement Campaigns, *J. Phys. Soc. Jpn.* 87(1), 014203 (2018)
122. R. Yokoyama, E. Ideguchi, G. S. Simpson, et al., Beta-gamma spectroscopy of the neutron-rich ^{150}Ba , *Prog. Theor. Exp. Phys.* 2018, 041D02 (2018)
123. J. Park, R. Krucken, D. Lubos, R. Gernhäuser, M. Lewitowicz, et al., β decays of the heaviest $N = Z - 1$ nuclei and proton instability of ^{97}In , *Phys. Rev. C* 97(5), 051301(R) (2018)
124. A. I. Morales, G. Benzoni, H. Watanabe, G. de Angelis, S. Nishimura, et al., Is seniority a partial dynamic symmetry in the first ng $9/2$ shell? *Phys. Lett. B* 781, 706 (2018)
125. J. L. Tain, J. Agramunt, D. S. Ahn, A. Algora, J. M. Allmond, et al., The BRIKEN Project: Extensive measurements of β -delayed neutron emitters for the astrophysical r process, *Acta Phys. Pol. B* 49(3), 417 (2018)
126. H. Wang, H. Otsu, H. Sakurai, D. S. Ahn, M. Aikawa, et al., Spallation reaction study for fission products in nuclear waste: Cross section measurements for ^{137}Cs and ^{90}Sr on proton and deuteron, *Phys. Lett. B* 754, 104 (2016)
127. H. Wang, H. Otsu, H. Sakurai, et al., Spallation reaction study for the long-lived fission product ^{107}Pd , *Prog. Theor. Exp. Phys.* 2017, 021D01 (2017)
128. S. Kawase, K. Nakano, Y. Watanabe, et al., Study of proton- and deuteron-induced spallation reactions on the long-lived fission product ^{93}Zr at 105 MeV/nucleon in inverse kinematics, *Prog. Theor. Exp. Phys.* 2017, 093D03 (2017)
129. Y. Kondo, T. Nakamura, R. Tanaka, R. Minakata, S. Ogoshi, et al., Nucleus ^{26}O : A barely unbound system beyond the drip line, *Phys. Rev. Lett.* 116(10), 102503 (2016)
130. Y. Togano, T. Nakamura, Y. Kondo, J. A. Tostevin, A. T. Saito, et al., Interaction cross section study of the two-neutron halo nucleus ^{22}C , *Phys. Lett. B* 761, 412 (2016)
131. J. W. Hwang, S. Kim, Y. Satou, N. A. Orr, Y. Kondo, et al., Single-neutron knockout from ^{20}C and the structure of ^{19}C , *Phys. Lett. B* 769, 503 (2017)
132. J. Yasuda, M. Sasano, R. G. T. Zegers, et al., Inverse kinematics (p, n) reactions studies using the WINDS slow neutron detector and the SAMURAI spectrometer, *Nucl. Instrum. Methods Phys. Res. Sect. B* 376, 393 (2016)
133. R. Shane, A. B. McIntosh, T. Isobe, et al., π S π RIT: A π time-projection chamber for symmetry-energy studies, *Nucl. Instrum. Methods Phys. Res. Sect. A* 784, 513 (2015)
134. K. Miki, H. Sakai, T. Uesaka, H. Baba, C. L. Bai, et al., Identification of the β^+ isovector spin monopole Resonance via the ^{208}Pb and ^{90}Zr ($t, ^3\text{He}$) Reactions at 300 MeV/u, *Phys. Rev. Lett.* 108(26), 262503 (2012)
135. K. Kisamori, S. Shimoura, H. Miya, S. Michimasa, S. Ota, et al., Candidate resonant tetra-neutron state populated by the ^4He ($^8\text{He}, ^8\text{Be}$) reaction, *Phys. Rev. Lett.* 116(5), 052501 (2016)
136. S. Noji, H. Sakai, N. Aoi, H. Baba, G. P. A. Berg, et al., Excitation of the isovector spin monopole resonance via the exothermic ^{90}Zr ($^{12}\text{N}, ^{12}\text{C}$) reaction at 175 MeV/u, *Phys. Rev. Lett.* 120(17), 172501 (2018)
137. S. Kawase, T. Uesaka, T. L. Tang, et al., Exclusive quasi-free proton knockout from oxygen isotopes at intermediate energies, *Prog. Theor. Exp. Phys.* 2018, 021D01 (2018)
138. S. Michimasa, M. Kobayashi, Y. Kiyokawa, S. Ota, D. S. Ahn, et al., Magic nature of neutrons in ^{54}Ca : First mass measurements of $^{55-57}\text{Ca}$, *Phys. Rev. Lett.* 121(2), 022506 (2018)
139. K. Tsukada, A. Enokizono, T. Ohnishi, K. Adachi, T. Fujita, et al., First elastic electron scattering from ^{132}Xe at the SCRIT facility, *Phys. Rev. Lett.* 118(26), 262501 (2017)
140. K. Morita, et al., RIKEN isotope separator on-line GARIS/IGISOL, *Nucl. Instrum. Methods Phys. Res. Sect. B* 70, 220 (1992)
141. D. Kaji, K. Morimoto, N. Sato, et al., Gas-filled recoil ion separator GARIS-II, *Nucl. Instrum. Methods Phys. Res. Sect. B* 317, 311 (2013)
142. Y. Ito, P. Schury, M. Wada, F. Arai, H. Haba, et al., First direct mass measurements of nuclides around $Z = 100$ with a multireflection time-of-flight mass spectrometer, *Phys. Rev. Lett.* 120(15), 152501 (2018)
143. T. Otsuka, R. Fujimoto, Y. Utsuno, B. A. Brown, M. Honma, and T. Mizusaki, Magic numbers in exotic nuclei and spin-isospin properties of the NN interaction, *Phys. Rev. Lett.* 87(8), 082502 (2001)